Carbohydrate Polymers 114 (2014) 344–351

Contents lists available at ScienceDirect

Carbohydrate Polymers

journal homepage: www.elsevier.com/locate/carbpol

Synthesis of thiolated glycosaminoglycans and grafting to solid surfaces

Alexander Köwitsch[a], Mauricio Jurado Abreu[a], Ankur Chhalotre[a], Martin Hielscher[b], Steffen Fischer[b], Karsten Mäder[c], Thomas Groth[a,*]

[a] Biomedical Materials Group, Institute of Pharmacy, Martin Luther University Halle-Wittenberg, Heinrich-Damerow-Strasse 4, D-06099 Halle Saale, Germany
[b] Institute of Plant and Wood Chemistry, Dresden University of Technology, Pienner Strasse 19, D-01737 Tharandt, Germany
[c] Pharmaceutical Technology Group, Institute of Pharmacy, Martin Luther University Halle-Wittenberg, Wolfgang-Langenbeck-Strasse 4, D-06099 Halle Saale, Germany

ARTICLE INFO

Article history:
Received 11 March 2014
Received in revised form 4 August 2014
Accepted 5 August 2014
Available online 23 August 2014

Keywords:
Glycosaminoglycan
Thiol-ene chemistry
Surface grafting
Microcontact printing (μcp)
Ellipsometry
Water contact angle measurements (WCA)

ABSTRACT

Glycosaminoglycans (GAGs) with varying degree of sulfation were chemically modified to obtain thiolated analogues (tGAGs) for subsequent surface grafting on vinyl-terminated self-assembled monolayers. Thiolation was achieved by the use of the disulfide containing crosslinker 3,3'-dithiobis(propanoic hydrazide) and subsequent reduction of the disulfide with dithiothreitol. Two different molar ratios of the crosslinker were used for conjugation. The tGAGs were characterized by ^{1}H-NMR, Raman and flow-field-flow-fractionation (A4F) to determine the chemical composition, structure and molecular weight of the products. Ellman's reagent was used to quantify the thiol concentration of tGAGs. The tGAGs were immobilized onto vinyl-terminated glass and silicon via thiol-ene reaction. This was achieved by homogeneous immobilization from solution as well as with microcontact printing and exposure to UV light. The results of water contact angle measurement (WCA), ellipsometry and confocal laser scanning microscopy (CLSM) demonstrated that the resulting surface coverage was dependent on the degree of thiolation of GAGs.

1. Introduction

Glycosaminoglycans (GAGs) are charged polysaccharides that contribute to tissue structure and function in vertebrates by their partly large molecular weight and ability to bind huge quantities of water, but also because of their inherent bioactivity (Varki, 2009). Heparin, hyaluronic acid (HA) and chondroitin sulfate (CS) represent linear, unbranched GAGs that are widely used in different biomedical applications. Heparin is composed of different disaccharide units mainly of D–glucuronic acid or L–iduronic acid linked to a D–glucosamine by a α (1–4) bond. The hexuronic acid can be sulfated at 2–*O* position whereas the glucosamine unit primarily carries a *N*–sulfation and a sulfation at 6–*O* position (Murugesan, Xie, & Linhardt, 2008). Heparin is found in secretory granula of mast cells and released during tissue injury. Heparin is well–known for its anticoagulant properties due to amplification of activity of anti–thrombin III, which plays a major role in clinical use. On the other hand, heparin binds also to adhesive proteins, cytokines and growth factors, which may affect their activity (Capila & Linhardt, 2002). Chondroitin sulfate is composed of disaccharides consisting of β (1–4) D–glucuronic acid and β (1–3) *N*–acetyl–D–galactosamine with potential *O*–sulfation. CS is the most abundant GAG in human body as a component of many different proteoglycans like aggrecan, versican, etc. (Kjellen & Lindahl, 1991). Besides the important role of chondroitin sulfate for compressive resistance of cartilage and other tissues (Nishimura et al., 1998), it plays also a role during fibrilization of collagen (Kvist et al., 2006) and may also interact with regulatory proteins for development and homeostasis of the nerve system (Rogers et al., 2011). In addition, it was also found that CS is a negative regulator of apoptosis by binding of tumor necrosis factor TNF–α (Xu et al., 2008). Hyaluronic acid consists of two repeating saccharide units β (1–4) D–glucuronic acid and β (1–3) *N*–acetyl–D–glucosamine. HA represents the only non–sulfated glycosaminoglycan and is widely used in medical approaches and cosmetic applications (Beasley, Weiss, & Weiss, 2009; Falcone & Berg, 2008; Volpi, Schiller, Stern, & Soltes,

* Corresponding author. Tel.: +49 0345 55 28460; fax: +49 0345 55 27379.
E-mail addresses: Alexander.Koewitsch@pharmazie.uni-halle.de (A. Köwitsch), Jurado.Abreu@hotmail.com (M. Jurado Abreu), Ankurchhalotre@gmail.com (A. Chhalotre), Martin.hielscher@forst.tu-dresden.de (M. Hielscher), Sfischer@forst.tu-dresden.de (S. Fischer), Karsten.maeder@pharmazie.uni-halle.de (K. Mäder), Thomas.groth@pharmazie.uni-halle.de (T. Groth).

http://dx.doi.org/10.1016/j.carbpol.2014.08.027
0144-8617/

2009). While CS is always linked to a core protein, HA is synthesized as a polysaccharide chain, which can be composed by thousands of disaccharide units which are able to bind to multiple aggrecan units which can lead to the formation of huge proteoglycan aggregates (Fraser, Laurent, & Laurent, 1997; Prehm, 1983). Beside the mechanical function of high molecular HA, this GAG has also important regulatory functions during inflammation, tumor progression and metastasis (Toole, 2009). Recently, HA has been chemically sulfated to alter its biological functions because sulfation has shown to be an important precondition for the interaction with growth factors and proteins of the extracellular matrix (Cencetti, Bellini, Longinotti, Martinelli, & Matricardi, 2011; Hintze et al., 2009).

The bioactivity of GAGs is connected to the interaction with a plethora of proteins that possess specific binding regions to bind them (Kjellen & Lindahl, 1991). Particularly adhesion and growth of cells is also regulated by the presence of GAGs in the surrounding extracellular matrix, but also on the surface of cells (Guillame-Gentil et al., 2010; Kuschert et al., 1999). Hence, surface modification of biomaterials with GAGs can provide specific adhesive cues for cells, like HA or CS to cell surface receptors CD 44 (Knudson, Aguiar, Hua, & Knudson, 1996; Iida et al., 1998) or act indirectly by binding of adhesive proteins with heparin–binding domains and integrins (Haugen, Mccarthy, Roche, Furcht, & Letourneau, 1992). The alteration of surface composition is often applied to control interaction of biomaterials with proteins and to mediate adhesion, proliferation and differentiation (Guillame-Gentil et al., 2010; Lee et al., 2013; Murugesan et al., 2008).

Hence, immobilization of some GAGs has been introduced to control the bioactivity of surfaces to promote binding of growth factors, adhesive proteins and direct behaviour of cells in scaffolds (Baldwin & Kiick, 2010; Gribova, Auzely-Velty, & Picart, 2012). However, different methods have been applied for GAG immobilization. Some require rather harsh methods of surface modification and subsequent covalent grafting of GAGs to the surface (Huang, Guduru, Xu, Vienken, & Groth, 2010). Other approaches use physical forces to adsorb GAGs that may lead to more loosely or irreversible immobilization (Aggarwal et al., 2013). For most of the recent techniques for covalent immobilization of GAGs several steps for surface modification or GAG treatment are necessary (Edlund, Danmark, & Albertsson, 2008). Another disadvantage might be that some methods are limited to oligosaccharides of GAGs (Chuang & Masters, 2009; Seo et al., 2007). We have shown recently that covalent grafting of pre–activated hyaluronan leads to functional material surfaces that guide binding of protein ligands like aggrecan but also adhesion of cells (Köwitsch et al., 2011). Here we focus on the use of free thiols as active moieties that allow direct covalent linkage of GAGs via click chemistry to vinyl groups or gold and expand the range of GAGs from hyaluronan to chondroitin sulfate, heparin and one sulfated hyaluronan. For thiolation of GAGs a disulfide containing crosslinker which exposes reactive hydrazide groups is applied. The latter has the benefit that the thiol group can be released or reactivated with a thiol-reducing agent and also uses less material than direct application of unprotected thiolation agents, which have to be used in excess thus resulting in a less effective thiolation (Hermanson, 1996; Shu, Liu, Luo, Roberts, & Prestwich, 2002). Beside the details of synthesis and characterization of derivates that differ also in degree of thiolation, we show their grafting to self–assembled monolayers via thiol–ene reaction and the generation of 2–D–structured surfaces via microcontact printing (μCP).

2. Materials and methods

2.1. Materials

Heparin (Hep) from porcine intestinal mucosa was purchased from Serva Electrophoresis GmbH (Heidelberg, Germany). Hyaluronic acid (HA) sodium salt (Mw 1.3 MDa) was provided by Kraeber & Co GmbH (Ellerbek, Germany). Low molecular weight HA (Mw 15 kDa) was obtained by acidic hydrolysis as reported previously (Köwitsch et al., 2011). Sulfated HA with a sulfation degree (D_{Sulf}) of 1.3 was provided by Innovent e.V. (Jena, Germany) (Hintze et al., 2009). Chondroitin sulfate A (from bovine trachea), N–Hydroxysuccinimide (NHS) and 6–aminofluorescein were obtained from Sigma–Aldrich (Schnelldorf, Germany). The dialysis bag (Spectra/Por membrane, Mw cutoff = 3500), D_2O and organic solvents were provided by Carl Roth GmbH (Germany). 3,3‘–dithiobis(propanoic hydrazide) (DTPH) was synthesized and analyzed as described before (Vercruysse, Marecak, Marecek, & Prestwich, 1997). 7–octenyldimethychlorosilane was purchased from ABCR GmbH & Co. KG (Karlsruhe, Germany), dithiothreitol (DTT) and 2–(N–Morpholino)ethanesulfonic acid monohydrate (MES) from VWR International GmbH (Dresden, Germany), tris(hydroxymethyl)aminomethane (TRIS) from Merck KGaA (Karlsruhe, Germany), 5,5′–dithiobis–(2–nitrobenzoic acid) (DTNB, Ellman‘s reagent) and 1–ethyl–3–(3–dimethylaminopropyl) carbodiimide hydrochloride (EDC) from Alfa Aesar (Karlsruhe, Germany).

2.2. Synthesis of thiolated glycosaminoglycans (tGAGs)

The synthesis of thiolated GAGs was performed with some modification according to a recent paper (Shu et al., 2002). All reactions were conducted at room temperature (RT). Briefly, 0.8 mmol of GAG (Hep, CS, HA, sHA) was dissolved in micropure water (80 mL). Then, 3,3‘–dithiobis(propanoic hydrazide) (DTPH, 0.2 mmol (representing 0.25 equivalents of the available —COOH groups) or 0.04 mmol (0.05 eq.)) was added to the stirring solution and the pH was adjusted to 4.75. Thereafter, EDC (0.5 mmol (for 0.25 eq.)/0.1 mmol (for 0.05 eq.)) was added while the pH was maintained at 4.75. After additional 3 h incubation 1 M NaOH was used to increase the pH to 7.0. Then, DTT (2.0 mmol) was added and the pH was raised to 8.5. The solution was stirred over night. Then, the pH of the reaction mixture was lowered to 3.5 before the solution was dialyzed against diluted HCl (pH 3.5) containing 100 mM NaCl for 2 days and against diluted HCl (pH 3.5) for 2 days. Finally, the solution was freeze–dried and a white product was obtained.

For the visualization via fluorescence microscopy the thiolated CS (tCS1.16) was labelled with 6–aminofluorescein. Therefore, 0.35 mmol of tCS1.16 was dissolved in 50 mL MES buffer (50 mM, pH 4.7). Then EDC (0.7 mmol) and NHS (0.7 mmol) were added and the solution was stirred for 1 h. The pH was adjusted to 7.0 and 9 mg of 6–aminofluorescein in 4 mL of DMSO was added. The container was wrapped in aluminium foil and stirred over night. Afterwards, the solution was acidified and dialyzed against diluted HCl (pH 3.5) for 5 days. Finally, the solution was freeze–dried and a pale yellow product was obtained.

2.3. Characterization of thiolated glycosaminoglycans (tGAGs)

The chemical structure of the thiolated GAGs was analyzed by ^{1}H–NMR (Varian Gemini 2000, Palo Alto, CA, USA). ^{1}H–NMR samples were dissolved in D_2O and measured with 256 repetitive scans at a frequency of 400 MHz to obtain the corresponding spectra.

Raman spectroscopy was performed with a Bruker MultiRam spectrometer (Ettlingen, Germany) equipped with a germanium diode as detector that is cooled with liquid nitrogen. A cw–Nd:YAG–laser with an exciting line of 1024 nm was applied as light source for the excitation of Raman scattering. The spectra were recorded over a range of 3500–0 cm^{-1} using an operating spectral resolution of 3 cm^{-1} and a laser power output of 125 mW. The thiol content of tGAGs was determined according to the results of the

UV–VIS (Specord 200, Analytik Jena AG, Jena, Germany) measurement using Ellman's reagent (Ellman, 1959). The molar absorption coefficient of 14,150 $M^{-1}cm^{-1}$ at 412 nm was used for the calculation of the total thiol concentration of the thiolated GAGs (Riddles, Blakeley, & Zerner, 1979). The thiol content was calculated by dividing the resulting thiol concentration (c_{SH}) by the theoretical thiol concentration ($c_{SH}{}^{th}$). The latter can be derived from the concentration of the solution used for the Ellman's assay (2 mg/mL) and the expected molecular weight of the thiolated GAG per disaccharide unit (Mw^{th}) ($c_{SH}{}^{th}$ = 2 mg/(Mw^{th} × 1 mL). The molecular weight and polydispersity of native and thiolated GAGs were determined by asymmetrical flow field–flow–fractionation (A4F) equipped with a Dawn EOS detector (Wyatt Technology, Santa Barbara, CA, USA) and a RI–Detector (Shodex, RI–101 Showa Denko Europe GmbH, Munich, Germany). All samples were measured at a concentration of 1 mg/mL in 50 mM NaCl. Molecular weights were calculated using Astra software (Wyatt Tech., Santa Barbara, CA, USA).

2.4. Surface modification

Glass cover slips (Menzel GmbH + Co KG, Braunschweig, Germany) were cleaned with 0.5 M NaOH in 96% ethanol for 2 h followed by excessive washing with micropure water (7 × 5 min) and dried in a stream of nitrogen. Silicon wafers (Silicon Materials, Kaufering, Germany) were treated with a solution of NH_4OH (27%), H_2O_2 (30%) and micropure water (1:1:5, v/v/v) at 70 °C for 15 min and subsequently washed with micropure water (7 × 5 min). Afterwards, the silicon wafers were also dried with a stream of nitrogen.

The vinyl–terminated surfaces were prepared according to manufacturer's instructions by the immersion of cleaned glass or silicon in an ethanolic solution of 7–octenyldimethychlorosilane (3%, v/v) for 24 h at room temperature. Thereafter, the solution was warmed to 35 °C for 3 h. Then the surfaces were rinsed with ethanol and washed with micropure water.

The reaction of the tGAGs with the vinyl–terminated glass or silicon surfaces was carried out in a UV light chamber (Bio–Link BLX, LTF Labortechnik GmbH & Co. KG, Wasserburg, Germany) at 365 nm (50 J cm^{-2}) in TRIS–HCl (50 mM, pH 7.4) for 4 h with a tGAG concentration of 2 mg/mL. The modified surfaces were washed and dried as mentioned above. A comparable approach was already used to create protein patterns on thiol–functionalized supports (Weinrich et al., 2010).

After immobilization of tGAGs, modified glass substrata were used for water contact angle measurements while the silicon substrata were employed for ellipsometry measurements.

2.5. Physical characterization of modified substrata

Static WCA measurements were performed with OCA 15+ device (Dataphysics, Filderstadt, Germany) utilizing the sessile drop method to measure the changes in wettability after surface modification of substrata and immobilization of tGAGs. Five droplets of 3 μL micropure water were applied to each sample and the obtained values were used to calculate means and standard deviations. The values mentioned herein represent the mean of at least two independent measurements which are composed of a minimum of three different samples each.

The layer thickness of the surface coatings with silane and GAGs on silicon was determined by ellipsometry (M–2000 V, J.A. Woollam Co. Inc., Lincoln, NE, USA) at the range of angles from 65° to 85°. A refractive index of 1.45 was used for the vinylsilane monolayer, while 1.41 was used for the tGAG coated samples (Booth, Vilt, McCabe, & Jennings, 2009) (Boddohi, Killingsworth, & Kipper, 2008; Booth et al., 2009). Measurements were performed three times on different locations of each surface (of three replicates) and averaged. The experimental data were analyzed with the WVase32 software provided with the equipment.

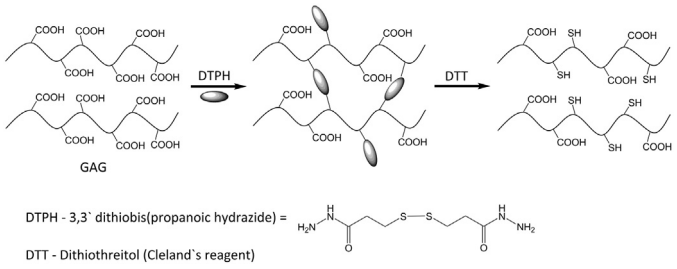

Fig. 1. Reaction scheme for the thiolation of glycosaminoglycans (GAGs).

2.6. Preparation and characterization of microcontact–printed surfaces

The polydimethylsiloxane (PDMS) stamps were made with Sylgard® 184 silicone elastomer kit (Dow Corning GmbH, Wiesbaden, Germany) according to the following conditions, which turned out to be most suitable for our experiments. The oven was preheated to 100 °C, whilst the curing agent and elastomer base were mixed for 5 min at a volume proportion of 1:10. The PDMS mixture was degassed in a vacuum chamber for 20 min to remove bubbles. The elastomer mix was injected into a mounted polycarbonate body, which was set on a casting station together with the silicon master (circular structures with ø = 80 μm, depth = 10 μm, elaborated by Tekniker, Eibar, Spain). The stamp was cured for 2 h at 100 °C. The cured stamp was cleaned with ethanol and micropure water. PDMS stamps were treated with oxygen plasma for 5 min (70 W/40 kHz, 0.08 mbar, 160 sccm/min O_2) (Walther et al., 2010). The plasma treated PDMS stamps were stored in micropure water to keep the wettability (Zhou, Ellis, & Voelcker, 2010).

For a reproducible microcontact printing a μcp–PVM–A printing module (GeSiM GmbH, Grosserkmannsdorf, Germany) was used, mounted on an inverted microscope (BIOLAB, Müller, Erfurt, Germany). The plasma treated stamp was inked by allowing 30 μL (5 mg/mL in 10 mM TRIS–HCl, pH 7.4) of fluorescein labelled tCS1.16 (FL–tCS1.16) to wet the stamp surface for 10 min in a closed humid chamber. Afterwards the stamp was blown dry with compressed air to remove excess of ink. Now the wetted stamp was mounted to the printing head of the PVM–A and the vinyl–terminated glass substrata was placed onto the printing stage. The printing time was set to 10 min according to previous findings in our lab. The former contact of the stamp and the glass substrate was assured by monitoring with an inverted microscope. After the stamp was removed from the surface, the printed substrate was irradiated at 365 nm for 10 min. Then the printed surface was washed with micropure water and TRIS–HCl. All microcontact printing steps were performed at room temperature.

3. Results and discussion

Here, a method that introduces thiol groups into the backbone of several glycosaminoglycans (GAGs) having different degree of sulfation was applied. To achieve thiolation of GAGs, the carboxylic acid groups of GAG were partly conjugated with DTPH, a disulfide containing crosslinker. Since the conjugation with DTPH results in a product that contains a disulfide bond and can lead also to crosslinking of GAGs, reduction with DTT is required to generate free thiol groups (Fig. 1). To explore the effect of the amount of applied crosslinker DTPH on thiolation degree and subsequent surface grafting, two different molar ratios of DTPH to GAG (1:4 and 1:20) were applied. Thiol–ene chemistry was used to generate

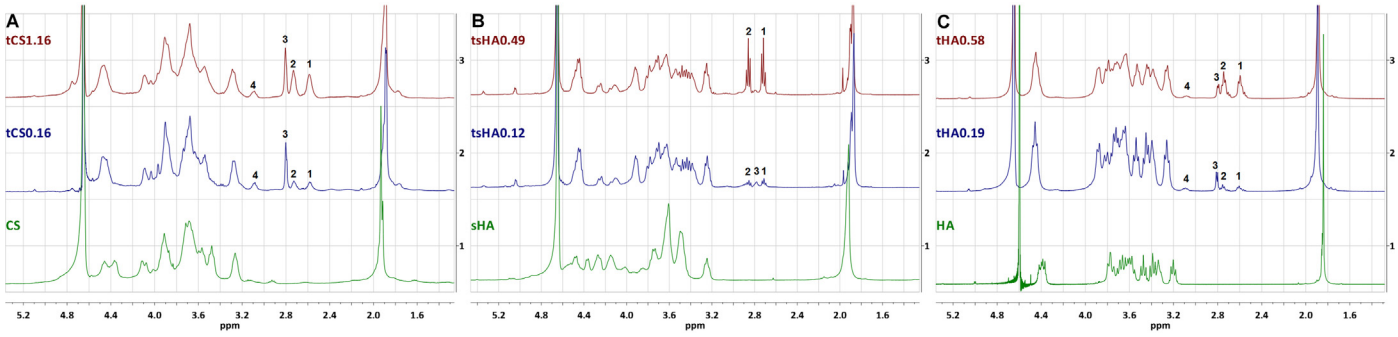

Fig. 2. ^{1}H–NMR spectra (400 MHz, D_2O) of derivatives of chondroitin sulfate (A), sulfated hyaluronic acid (B) and hyaluronic acid (C).

covalently immobilized GAG–substrata. Thus, we grafted the tGAGs to vinyl–terminated surfaces by means of homogeneous immobilization from solution or by microcontact printing (μcp) to generate microstructured substrata. The obtained surfaces were characterized by physical methods, such as wettability and coating thickness, to show the change of surface properties.

3.1. Synthesis and characterization of thiolated glycosaminoglycans

Nuclear magnetic resonance spectroscopy (NMR) was utilized to detect the molecular changes resulting from the grafting of DTPH to the GAGs. The exemplary spectra of the thiolated and native GAG derivatives are depicted in Fig. 2. ^{1}H–NMR spectra can be used to calculate the amount of crosslinker conjugated to the carboxylic acid groups of GAGs comparing the peak areas of the singlet of the methyl group of the acetamide (δ 1.9) with the new adsorptions of the four hydrogens belonging to the methylene groups (—CH_2CH_2S—) of the introduced crosslinker DTPH. When the disulfide was successfully cleaved by DTT, then the methylene groups have a chemical shift at δ 2.60 for HA (—CH_2CH_2SH, 1 in Fig. 2C) and δ 2.75 for HA (—CH_2CH_2SH, 2 in Fig. 2C), respectively. If the disulfide was not cleaved the methylene groups show peaks at δ 2.80 (–CH_2CH_2S–, 3 in Fig. 2C) and at δ 3.08 (—CH_2CH_2S—, 4 in Fig. 2C) in case of HA. Since the peak with a chemical shift around δ 3.08 is very broad and cannot be integrated with accuracy for the tGAGs, the resulting degree of substitution (DS) is probably slightly smaller for all tGAGs. Nevertheless, the DS was calculated from ^{1}H–NMR spectra for HA, sHA and CS, which have a constant repetition of the same disaccharide units in the carbohydrate chain. By contrast, heparin does not have exactly one acetyl group per disaccharide unit, which did not allow the calculation of DS. It has been shown previously that DS can be controlled by the variation of the molar ratios of GAG/DTPH/EDC and different reaction times. For example, 27–67% substitution of the carboxylic acid groups of a HA with a molecular weight of 250 kDa has been reported by Shu et al. (2002).

The results of ^{1}H—NMR spectroscopy of tHA0.58 indicate that a total amount of 31% of carboxyl groups reacted with DTPH of the sample with a ratio of 1:4 of DTPH/—COOH and 13% of the sample with ratio of 1:20 of DTPH/—COOH, respectively. The results of calculations of DS from ^{1}H—NMR spectra are shown in Table 1. It is clearly evident that all DTPH molecules seem to react with the corresponding GAG when a DTPH/—COOH ratio of 1:20 was used for the thiolation since the resulting DS was between 10–13%. By contrast, in case of a starting DTPH/—COOH ratio of 1:4, a lower than expected DS between 31–41% was obtained, without consideration of heparin. This implies that the access of the carboxylic acid groups is hindered when a higher DS shall be achieved. One reason for that could be the sterical hindrance because of aggregation of GAGs or the crosslinking with DTPH.

A common method for the analysis of free thiols is Raman spectroscopy. The S—H stretching vibration is located between 2600–2535 cm^{-1} and gives a strong signal in Raman spectra (Socrates, 2001). During investigations with Raman spectroscopy the specific adsorption band at 2585–2560 cm^{-1} (* in Fig. 3) in the spectra of tCS1.16 and tHA0.58 were found, but not for the other tGAG. This might be explained by the lower sensitivity of Raman compared to the UV–VIS measurements with Ellman's reagent. Nevertheless, the introduction of the disubstituted hydrazide by the reaction with DTPH was detected by a specific adsorption of the carbonyl double bond (Amide I) in the region 1750–1700 cm^{-1} (+ in Fig. 3) whereas for the native GAGs the adsorption bands visible in the region 1680–1600 cm^{-1} (o in Fig. 3) are attributed to the carbonyl stretch of the free carboxylic acid (full spectra in supplementary data). This new band was also visible for tHep0.29, which confirmed the successful conjugation of DTPH to heparin.

Since the Raman spectroscopy was not sensitive enough to verify the presence of free thiols in all tGAGs, Ellman's Reagent (DTNB) was used to measure the exact thiol concentration of the products by UV–VIS spectrometry (Table 1). The thiol content was calculated as mentioned in the methods section. Thus, the thiol content directly displays how many free thiols exist per repeating disaccharide of the corresponding GAG. If the bifunctional crosslinker DTPH would react quantitatively and on both ends it would be expected to obtain tGAGs with a substitution of 50% (DTPH/—COOH ratio = 1:4) or 10% (DTPH/—COOH ratio = 1:20), respectively. The results in Table 1 show that with a rising amount of DTPH not only a higher DS but also an increase in free thiols was obtained. After conjugation with the two different DTPH ratios, most thiols were found for tCS in both cases. In case of lower starting amounts of DTPH all resulting tGAGs had similar thiol concentrations. This

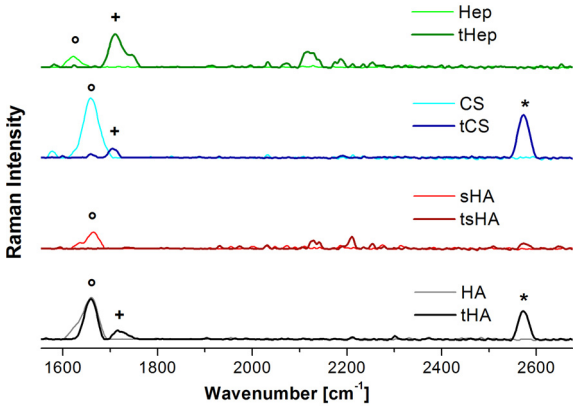

Fig. 3. FT Raman spectra (2600–1600 cm^{-1}) of thiolated GAGs showing the–SH stretch (*) and the C = O adsorption bands of the free carboxylic acid groups (°) and the disubstituted hydrazide (+).

Table 1
Degree of substitution (DS) and thiol concentration (c_{SH})of thiolated glycosaminoglycans calculated based on results of ^{1}H–NMR and Ellman's assay.

Sample	tHep0.11	tHep0.29	tCS0.16	tCS1.16	tsHA0.12	tsHA0.49	tHA0.19	tHA0.58
Degree of substitution (DS)	n.d.	n.d.	10%	41%	13%	40%	13%	31%
Thiol conc.	0.11/	0.29/	0.16/	1.16/	0.12/	0.49/	0.19/	0.58/
[x10^{-3}mol/L]/thiol content	3.7%	10.0%	4.4%	30.7%	3.2%	13.3%	3.9%	12.2%

was even more prominent when comparing the thiol content (3.2–4.4%), which also includes the different molecular weights of GAGs. For tGAGs with a higher DS significantly more free thiols were obtained in case of tCS1.16, while the other tGAGs gathered in a rather comparable range. Considering the DS that resulted from the ^{1}H–NMR the proportion of disulfides of DTPH can be estimated that was cleaved by DTT to generate free thiol groups. For tCS1.16 a thiol content of 30.7% and a DS of 41% was obtained, which means that around 75% of the introduced disulfides of DTPH were reduced to free thiols by DTT. Since the DS for tHep could not obtained by spectroscopy, this ratio is highest for the tCS samples (44%/75%) and lowest for the tsHA analogues (25%/33%). An important factor that controls DS could be the conformation of the GAG prior to reduction of the disulfide by DTT. The fact that not all of the disulfides could be cleaved to free thiols by reduction with DTT led obviously to an increase in molecular weight as a result of the intermolecular crosslinking of GAG chains (Table 2). It can be concluded that an increase of DS resulted in a product with a higher molecular weight (Mw). This trend is more pronounced when the above mentioned ratio of the thiol content and the DS is decreasing. The lowest increase in Mw and also polydispersity was shown for tCS1.16 which is comprehensible taking into account the fact that the ratio of the thiol content and the DS was highest (75%) in this sample. The less disulfides are cleaved, the higher the conjugation of tGAGs and the resulting Mw. In particular, tHA0.58 with a high degree of substitution (DS) showed a large increase in molecular weight even it had a comparable thiol content/DS ratio as tsHA0.49, which indicates that the sulfation influences the final Mw of the product. The presence of equally charged groups leads to more intra– and intermolecular repulsion. The non–sulfated HA is the least charged GAG and thus not repelling the hydrophobic part of DTPH as much as the more negatively charged sulfated GAGs. As a consequence the conformation of the crosslinked HA is more closed and inaccessible for the reduction of the disulfide by DTT.

3.2. Characterization of glycan-modified substrata

The immobilization of tGAGs was carried out on vinyl–terminated self–assembled monolayer (SAM) via the thiol–ene reaction that was initiated by UV–treatment. The covalent S—C—bond formation between the alkene and the thiol group is difficult to detect with spectroscopy due to their low concentration on the substrate and the high sulfur content of GAGs (except HA). Therefore, indirect measurement verifying the success of immobilization was performed with surface sensitive methods that measure wetting properties (water contact angle, WCA) and layer thickness (ellipsometry).

The results of water contact angle (WCA) measurements depicted in Fig. 4 show a considerable increase of WCA, when the hydrophilic cleaned glass cover slips were modified with a vinyl–terminated SAM resulting in a WCA of about 95°. This result is in good accordance to a previous study on surface modification with silanes having the same functional group (Faucheux, Schweiss, Lutzow, Werner, & Groth, 2004). The subsequent immobilization of tGAGs decreased the WCA because of the hydrophilic nature of GAGs, but to a different extent. First of all, only a moderate decrease of WCA was observed. This was rather unexpected due to the presence of polar hydroxyl and charged carboxylic and sulfate groups in the GAGs. However, a part of the carboxylic groups was converted and the introduction of DTPH will also decrease the hydrophilicity of GAGs to some extent. In addition steric hindrance during grafting–to may also limit surface density of GAG to some extent as it has been described previously for other molecules (Zajac & Chakrabarti, 1995). A strong evidence for thiol–ene reaction during the immobilisation of tGAG was that the observed decrease of WCA was always more pronounced in case of the higher thiolated GAGs. This indicates that a higher concentration of reactive thiols leads to more surface coverage due to the increased covalent binding of GAGs. When the degree of sulfation of tGAGs was compared it was also evident that heparin (D_{Sulf} = 1.6), which is the most sulfated GAG, yielded the lowest WCA were measured. Nevertheless, the tCS immobilization produced more wettable substrata than tsHA even the sulfation degree of sHA (D_{Sulf} = 1.3) was higher than that of CS (D_{Sulf} = 0.8). It was assumed that the higher concentration of free thiols in tCS samples compared to tsHA samples might lead to an enhanced surface coverage. Despite the conjugation of DTPH to the carboxylic groups of all GAGs also non–sulfated HA led to more hydrophilic surfaces indicating that tHA0.58 was able to cover the surface to a higher extent than sHA0.49, which

Table 2
Molecular weight and Polydispersity index (PDI) of glycosaminoglycans.

Sample	Mw (kDa)	PDI (Mw/Mn)
Heparin	15	1.1
tHep0.11	17	1.5
tHep0.29	28	1.5
CS	25	1.4
tCS0.16	27	1.4
tCS1.16	30	1.5
sHA (D_{Sulf} = 1.3)	12–17[a]	2.0[a]
tsHA0.12	24	1.9
tsHA0.49	38	1.9
LMWHA	12	1.2
tHA0.19	14	1.4
tHA0.58	64	2.7

[a] Determined by gel permeation chromatography (GPC)

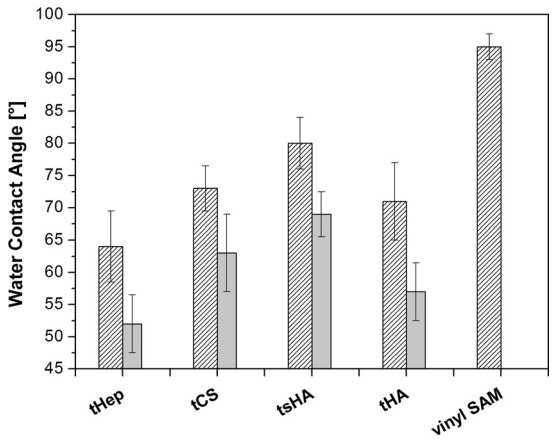

Fig. 4. Change of wettability for thiolated GAGs with different degree of substitution compared to vinyl–terminated glass (thiol concentration of tGAGs: hatched–tHep0.11, tCS0.16, tsHA0.12, tHA0.19; grey–tHep0.29, tCS1.16, tsHA0.49, tHA0.58).

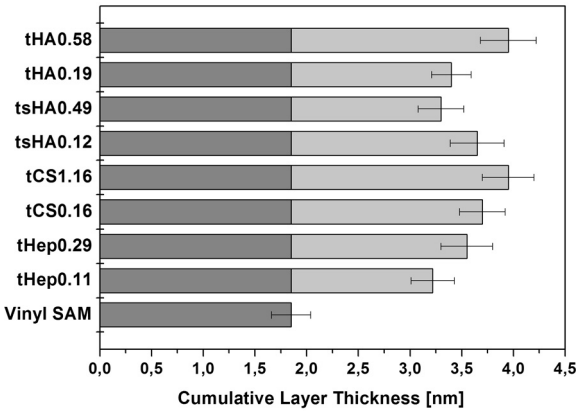

Fig. 5. Cumulative layer thickness of thiolated GAGs compared to vinyl–terminated silicon measured by ellipsometry.

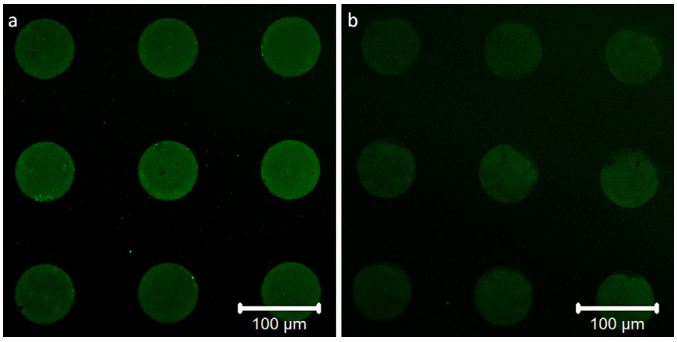

Fig. 6. Confocal laser scanning microscopy micrographs of FL–tCS1.16 printed onto vinyl–terminated glass before (a) and after (b) additional washing with TRIS–HCl (pH 7.4).

should be more hydrophilic because of sulfate groups. The molecular weight of tGAGs directly influences the wettability too, because a larger molecule can cover a larger surface area than a smaller one. Here, tHA0.58 possessed the highest Mw which may explain the lower WCA compared to the sulfated GAGs. Overall, it seems that the immobilization of tGAGs on vinyl–terminated SAM did not lead to complete surface coverage. This may be due to steric hindrance of adjacent GAG molecules during the grafting to the vinyl SAM, which could prevent the attachment of additional molecules. Another obstacle may also be the more hydrophobic nature of the surface that may also reduce the interaction with hydrophilic GAGs and last but not least a lower efficiency of the UV–initiated thiol–ene reaction (Jeyachandran, Mielezarski, Rai, & Mielczarski, 2009; Karlsson, Edfors-Lilja, & Bjornsson, 2000; Rouse, Whateley, Thomas, & Eccleston, 2007).

Ellipsometry is a useful tool to determine the thickness of coatings on reflective substrata like silicon, which is measured by the induced change of the polarization state of light reflected on the surface (Tompkins & Irene, 2005). All measurements were conducted under dry laboratory conditions at room temperature. Therefore, no swelling of the coating material can be expected. The oxide layer of silicon was measured and set as the basal layer. The thickness of the following layers includes the vinyl–terminated SAM plus tGAG layer and is shown in Fig. 5. The thickness of the vinyl–terminated SAM of 1.85 nm is in correspondence with results of silanes with similar length (Wasserman, Tao, & Whitesides, 1989). In general, the immobilization of the tGAGs resulted in surface coatings with a thickness between 1.37 nm (tHep0.11) and 2.1 nm (tCS1.16). There were no major differences in layer thickness between the different GAGs, which might be due to the fact that the experiments were performed in a dry state. Nevertheless, a higher thiol content of the tGAGs led also to higher layer thickness except for the tsHA substrata. Ellipsometry is based on an integral measurement of a comparatively large surface area. Hence, the resulting layer thickness always incorporates also vacant areas due to the incomplete surface coverage that has been also deduced from WCA measurements. The immobilization of tCS1.16 and tHA0.58 on vinyl–terminated silicon resulted in the most pronounced thickness increase of about 2.1 nm. This could be correlated to the concentration of free thiols, which are highest for these tGAGs. The lowest thickness was measured for substrata coated with the tHep0.11 (1.37 nm) surfaces. To get an idea of the dimensions of thickness measured with ellipsometry one has to consider that a single saccharide ring has a diameter of around 1 nm. Yeh et al. determined the height of HA in dry state with AFM measurements to 0.54 nm (Yeh & Luo, 2004). Layer by layer studies of heparin and chitosan also showed that single heparin layers had a concentration dependent thickness between 0.5 nm and 2 nm when measured by ellipsometry (Boddohi et al., 2008). In the present study one has to consider also the size of the crosslinker (DTPH) that was introduced to the GAGs. From these considerations one can assume that the surface grafting of tGAGs resulted in a side–on configuration perhaps including some loopy conformation of GAGs. This is also more probable for tGAGs with lower thiol content, because they have less covalent links to the substratum. On the other hand, it is conceivable that tGAGs might not be strictly immobilized in monolayers because they can still present free thiol groups after immobilization enabling them to bind to other tGAGs chains in solution via disulfide formation.

In addition to the characterization of surface properties also bioactivity of the surface-immobilized tGAGs was characterized by studying adhesion and metabolic activity of fibroblasts seeded in serum containing medium. Here the idea was that sulfated GAGs like heparin can bind adhesive proteins like fibronectin and vitronectin present in plasma that possess heparin-binding domains and thus support cell adhesion (Steele, Johnson, & Underwood, 1992). On the other hand, cells possess also adhesion receptors like CD 44 that can recognize certain GAGs like HA directly (Dickinson, Ho, Wang, Stebe, & Gerecht, 2010). Since thiolation changes the chemical structure and also accessibility of GAG chains, it was assumed that reduced adhesion and spreading of cells indicates a lower bioactivity of thiolated GAGs. Accordingly, the adhesion of cells was studied with phase contrast microscopy while metabolic activity of cells was measured with Qblue® assay after 24 h and 48 h. Results of this study are shown in supplementary data with Figs. S1, S2 and S3. Fig. S1 shows that for most of tGAG-coated surfaces a significant increase in metabolic activity of fibroblasts was observed within this time period. However, it was found that substrata coated with highly thiolated tCS1.16 and tHA0.58 showed a noticeable lower metabolic activity than the other tGAGs. These findings were also confirmed by cell adhesion studies after 24 h (Fig. S2) and 48 h (Fig. S3). Here it was also evident that the number of adhering cells on highly thiolated tCS1.16 and tHA0.58 were lower at both time points. This indicates a potential lower bioactivity in case of too high thiolation of GAGs.

3.3. *Making of microcontact–printed surfaces with thiolated GAGs*

As an additional method we applied microcontact printing (μcp) to create GAG-textured substrata. In an exemplary approach we used fluorescein-labelled tCS (FL–tCS1.16) as ink for soft lithography and visualized the resulting prints by confocal laser scanning microscopy. In Fig. 6 the result of the print is depicted prior and after washing with TRIS–HCl (pH 7.4). It can be seen that also after the additional washing step with buffered solution the printed

structures remain on the glass surface, even some unbound FL–tCS1.16 from the periphery of the prints was removed. That makes them good candidates for subsequent cell migration or co–culture studies to explore the specific effect of the different printed tGAGs.

It was found that not only the FL–tCS1.16 could be easily transferred to the vinyl–terminated glass surfaces by μcp but also fluorescein labelled analogues of tHA and tHep. In addition to the result for a PDMS stamp with 80 μm circular structures which is depicted in Fig. 6 the labelled tGAGs can be also applied to stamps with smaller sized structures to generate other surface structures.

4. Conclusion

In this work four GAGs were thiolated with two different degrees of substitution. The accessibility of the carboxylic acid groups decreased when an increased amount of DTPH was used. The surface grafting of tGAGs could be achieved in a homogeneous manner as well as in a microstructured way by microcontact printing. It was found that the surface coverage was improved with a higher degree of thiolation and an increased molecular weight of the tGAGs. The resulting glycanized surfaces presented an increase in wettability and layer thickness. The wettability of the homogeneous coated substrata seemed to be dependent on the sulfation degree and molecular weight of the immobilized tGAGs. Studies with human fibroblasts showed also that surface coatings with tGAGs were bioactive although a higher thiolation degree of tCS and tHA reduced cell activity to some extent. In conclusion, the thiol–ene reaction seems to be a facile method to graft thiolated GAGs to vinyl–terminated or gold substrata. Such surface modified with different GAGs may be useful for quantitative studies of protein-GAG interaction with surface plasmon resonance or quartz microbalance (Altgarde et al., 2013; Yagi et al., 2012). On the other hand, the important role of GAGs during inflammation and tumor development may also open applications of GAG modified surfaces for studies on cell adhesion and migration (Dickinson et al., 2010). Furthermore, the detection of specific interaction partners or cell mobility is an interesting task that could be addressed with biosensing devices coated or structured with GAGs. HA, for instance, has shown to have a promoting effect on metastatic cancer cells that could be studied with such biosensors (Afify, Purnell, & Nguyen, 2009).

Acknowledgements

This work was supported by the European Union Seventh Framework Programme (FP7/2007–2013) under grant agreement no. NMP4–SL–2009–229292 ("Find & Bind"). The authors also want to thank the Interdisciplinary Center for Material Sciences in Halle (Germany) for the opportunity to use the ellipsometer and the plasma cleaner. We are grateful for support of this work by the micro and nano manufacture unit at IK4–Tekniker (Spain) for the silicon master preparation and Innovent e.V. (Germany) for providing the sulfated hyaluronic acid. The authors thank Ute Mentzel for her support of the A4F experiments.

Appendix A. Supplementary data

Supplementary data associated with this article can be found, in the online version, at http://dx.doi.org/10.1016/j.carbpol.2014.08.027.

References

Afify, A., Purnell, P., & Nguyen, L. (2009). Role of CD44s and CD44v6 on human breast cancer cell adhesion, migration, and invasion. *Experimental and Molecular Pathology*, *86*(2), 95–100.

Aggarwal, N., Altgarde, N., Svedhem, S., Zhang, K., Fischer, S., & Groth, T. (2013). Effect of molecular composition of heparin and cellulose sulfate on multilayer formation and cell response. *Langmuir*, *29*(45), 13853–13864.

Altgarde, N., Nileback, E., de Battice, L., Pashkuleva, I., Reis, R. L., Becher, J., et al. (2013). Probing the biofunctionality of biotinylated hyaluronan and chondroitin sulfate by hyaluronidase degradation and aggrecan interaction. *Acta Biomaterialia*, *9*(9), 8158–8166.

Baldwin, A. D., & Kiick, K. L. (2010). Polysaccharide-modified synthetic polymeric biomaterials. *Biopolymers*, *94*(1), 128–140.

Beasley, K. L., Weiss, M. A., & Weiss, R. A. (2009). Hyaluronic acid fillers: A comprehensive review. *Facial Plastic Surgery*, *25*(2), 86–94.

Boddohi, S., Killingsworth, C. E., & Kipper, M. J. (2008). Polyelectrolyte multilayer assembly as a function of pH and ionic strength using the polysaccharides chitosan and heparin. *Biomacromolecules*, *9*(7), 2021–2028.

Booth, B. D., Vilt, S. G., McCabe, C., & Jennings, G. K. (2009). Tribology of monolayer films: Comparison between n-alkanethiols on gold and n-alkyl trichlorosilanes on silicon. *Langmuir*, *25*(17), 9995–10001.

Capila, I., & Linhardt, R. J. (2002). Heparin—protein interactions. *Angewandte Chemie-International Edition*, *41*(3), 391–412.

Cencetti, C., Bellini, D., Longinotti, C., Martinelli, A., & Matricardi, P. (2011). Preparation and characterization of a new gellan gum and sulphated hyaluronic acid hydrogel designed for epidural scar prevention. *Journal of Materials Science-Materials in Medicine*, *22*(2), 263–271.

Chuang, T. W., & Masters, K. S. (2009). Regulation of polyurethane hemocompatibility and endothelialization by tethered hyaluronic acid oligosaccharides. *Biomaterials*, *30*(29), 5341–5351.

Dickinson, L. E., Ho, C. C., Wang, G. M., Stebe, K. J., & Gerecht, S. (2010). Functional surfaces for high-resolution analysis of cancer cell interactions on exogenous hyaluronic acid. *Biomaterials*, *31*(20), 5472–5478.

Edlund, U., Danmark, S., & Albertsson, A. C. (2008). A strategy for the covalent functionalization of resorbable polymers with heparin and osteoinductive growth factor. *Biomacromolecules*, *9*(3), 901–905.

Ellman, G. L. (1959). Tissue sulfhydryl groups. *Archives of Biochemistry and Biophysics*, *82*(1), 70–77.

Falcone, S. J., & Berg, R. A. (2008). Crosslinked hyaluronic acid dermal fillers: a comparison of rheological properties. *Journal of Biomedical Materials Research Part A*, *87A*(1), 264–271.

Faucheux, N., Schweiss, R., Lutzow, K., Werner, C., & Groth, T. (2004). Self-assembled monolayers with different terminating groups as model substrates for cell adhesion studies. *Biomaterials*, *25*(14), 2721–2730.

Fraser, J. R. E., Laurent, T. C., & Laurent, U. B. G. (1997). Hyaluronan: Its nature, distribution, functions and turnover. *Journal of Internal Medicine*, *242*(1), 27–33.

Gribova, V., Auzely-Velty, R., & Picart, C. (2012). Polyelectrolyte multilayer assemblies on materials surfaces: From cell adhesion to tissue engineering. *Chemistry of Materials*, *24*(5), 854–869.

Guillame-Gentil, O., Semenov, O., Roca, A. S., Groth, T., Zahn, R., Vörös, J., et al. (2010). Engineering the extracellular environment: Strategies for building 2D and 3D cellular structures. *Advanced Materials*, *22*(48), 5443–5462.

Haugen, P. K., Mccarthy, J. B., Roche, K. F., Furcht, L. T., & Letourneau, P. C. (1992). Central and peripheral neurite outgrowth differs in preference for heparin-binding versus integrin-binding sequences. *Journal of Neuroscience*, *12*(6), 2034–2042.

Hermanson, G. T. (1996). *Bioconjugate Techniques*. San Diego: Elsevier Science.

Hintze, V., Moeller, S., Schnabelrauch, M., Bierbaum, S., Viola, M., Worch, H., et al. (2009). Modifications of hyaluronan influence the interaction with human bone morphogenetic protein-4 (hBMP-4). *Biomacromolecules*, *10*(12), 3290–3297.

Huang, X. J., Guduru, D., Xu, Z. K., Vienken, J., & Groth, T. (2010). Immobilization of heparin on polysulfone surface for selective adsorption of low-density lipoprotein (LDL). *Acta Biomaterialia*, *6*(3), 1099–1106.

Iida, J., Meijne, A. M. L., Oegema, T. R., Yednock, T. A., Kovach, N. L., Furcht, L. T., et al. (1998). A role of chondroitin sulfate glycosaminoglycan binding site in alpha(4)beta(1) integrin-mediated melanoma cell adhesion. *Journal of Biological Chemistry*, *273*(10), 5955–5962.

Jeyachandran, Y. L., Mielezarski, E., Rai, B., & Mielczarski, J. A. (2009). Quantitative and qualitative evaluation of adsorption/desorption of bovine serum albumin on hydrophilic and hydrophobic surfaces. *Langmuir*, *25*(19), 11614–11620.

Karlsson, M., Edfors-Lilja, I., & Bjornsson, S. (2000). Binding and detection of glycosaminoglycans immobilized on membranes treated with cationic detergents. *Analytical Biochemistry*, *286*(1), 51–58.

Kjellen, L., & Lindahl, U. (1991). Proteoglycans—structures and interactions. *Annual Review of Biochemistry*, *60*, 443–475.

Knudson, W., Aguiar, D. J., Hua, Q., & Knudson, C. B. (1996). CD44-anchored hyaluronan-rich pericellular matrices: An ultrastructural and biochemical analysis. *Experimental Cell Research*, *228*(2), 216–228.

Köwitsch, A., Yang, Y., Ma, N., Kuntsche, J., Mäder, K., & Groth, T. (2011). Bioactivity of immobilized hyaluronic acid derivatives regarding protein adsorption and cell adhesion. *Biotechnology and Applied Biochemistry*, *58*(5), 376–389.

Kuschert, G. S. V., Coulin, F., Power, C. A., Proudfoot, A. E. I., Hubbard, R. E., Hoogewerf, A. J., et al. (1999). Glycosaminoglycans interact selectively with chemokines and modulate receptor binding and cellular responses. *Biochemistry*, *38*(39), 12959–12968.

Kvist, A. J., Johnson, A. E., Morgelin, M., Gustafsson, E., Bengtsson, E., Lindblom, K., et al. (2006). Chondroitin sulfate perlecan enhances collagen fibril formation—Implications for perlecan chondrodysplasias. *Journal of Biological Chemistry*, *281*(44), 33127–33139.

Lee, S.-Y., Yun, Y.-P., Song, H.-R., Chun, H. J., Yang, D. H., Park, K., et al. (2013). The effect of titanium with heparin/BMP-2 complex for improving osteoblast activity. *Carbohydrate Polymers*, *98*(1), 546–554.
Murugesan, S., Xie, J., & Linhardt, R. J. (2008). Immobilization of heparin: Approaches and applications. *Current Topics in Medicinal Chemistry*, *8*(2), 80–100.
Nishimura, M., Yan, W. Q., Mukudai, Y., Nakamura, S., Nakamasu, K., Kawata, M., et al. (1998). Role of chondroitin sulfate hyaluronan interactions in the viscoelastic properties of extracellular matrices and fluids. *Biochimica Et Biophysica Acta-General Subjects*, *1380*(1), 1–9.
Prehm, P. (1983). Synthesis of hyaluronate in differentiated teratocarcinoma cells—Characterization of the synthase. *Biochemical Journal*, *211*(1), 181–189.
Riddles, P. W., Blakeley, R. L., & Zerner, B. (1979). Ellman's reagent: 5,5'-dithiobis(2-nitrobenzoic acid)—a reexamination. *Analytical Biochemistry*, *94*(1), 75–81.
Rogers, C. J., Clark, P. M., Tully, S. E., Abrol, R., Garcia, K. C., Goddard, W. A., et al. (2011). Elucidating glycosaminoglycan-protein-protein interactions using carbohydrate microarray and computational approaches. *Proceedings of the National Academy of Sciences of the United States of America*, *108*(24), 9747–9752.
Rouse, J. J., Whateley, T. L., Thomas, M., & Eccleston, G. M. (2007). Controlled drug delivery to the lung: Influence of hyaluronic acid solution conformation on its adsorption to hydrophobic drug particles. *International Journal of Pharmaceutics*, *330*(1–2), 175–182.
Seo, J. H., Adachi, K., Lee, B. K., Kang, D. G., Kim, Y. K., Kim, K. R., et al. (2007). Facile and rapid direct gold surface immobilization with controlled orientation for carbohydrates. *Bioconjugate Chemistry*, *18*(6), 2197–2201.
Shu, X. Z., Liu, Y. C., Luo, Y., Roberts, M. C., & Prestwich, G. D. (2002). Disulfide cross-linked hyaluronan hydrogels. *Biomacromolecules*, *3*(6), 1304–1311.
Socrates, G. (2001). *Infrared and Raman characteristic group frequencies: Tables and charts*. New York: Wiley. Chichester
Steele, J. G., Johnson, G., & Underwood, P. A. (1992). Role of serum vitronectin and fibronectin in adhesion of fibroblasts following seeding onto tissue-culture polystyrene. *Journal of Biomedical Materials Research*, *26*(7), 861–884.
Tompkins, H. G., & Irene, E. A. (2005). *Handbook of ellipsometry*. Heidelberg Germany: Norwich, NY,William Andrew Pub. Springer.
Toole, B. P. (2009). Hyaluronan-CD44 interactions in cancer: Paradoxes and possibilities. *Clinical Cancer Research*, *15*(24), 7462–7468.
Varki, A. (2009). *Essentials of glycobiology*. Cold Spring Harbor N. Y.: Harbor Laboratory Press.
Vercruysse, K. P., Marecak, D. M., Marecek, J. F., & Prestwich, G. D. (1997). Synthesis and in vitro degradation of new polyvalent hydrazide cross-linked hydrogels of hyaluronic acid. *Bioconjugate Chemistry*, *8*(5), 686–694.
Volpi, N., Schiller, J., Stern, R., & Soltes, L. (2009). Role, metabolism chemical modifications and applications of hyaluronan. *Current Medicinal Chemistry*, *16*(14), 1718–1745.
Walther, F., Drobek, T., Gigler, A. M., Hennemeyer, M., Kaiser, M., Herberg, H., et al. (2010). Surface hydrophilization of SU-8 by plasma and wet chemical processes. *Surface and Interface Analysis*, *42*(12–13), 1735–1744.
Wasserman, S. R., Tao, Y. T., & Whitesides, G. M. (1989). Structure and reactivity of alkylsiloxane monolayers formed by reaction of alkyltrichlorosilanes on silicon substrates. *Langmuir*, *5*(4), 1074–1087.
Weinrich, D., Kohn, M., Jonkheijm, P., Westerlind, U., Dehmelt, L., Engelkamp, H., et al. (2010). Preparation of biomolecule microstructures and microarrays by thiol-ene photoimmobilization. *ChemBioChem*, *11*(2), 235–247.
Xu, C. X., Jin, H., Chung, Y. S., Shin, J. Y., Woo, M. A., Lee, K. H., et al. (2008). Chondroitin sulfate extracted from the Styela clava tunic suppresses TNF-alpha-induced expression of inflammatory factors VCAM-1 and NOS by blocking Akt/NF-kappa B signal in JB6 cells. *Cancer Letters*, *264*(1), 93–100.
Yagi, M., Murray, J., Strand, K., Blystone, S., Interlandi, G., Suda, Y., et al. (2012). Heparin modulates the conformation and signaling of platelet integrin alpha IIb beta 3. *Thrombosis Research*, *129*(6), 743–749.
Yeh, M. L., & Luo, Z. P. (2004). The structure of proteoglycan aggregate determined by atomic force microscopy. *Scanning*, *26*(6), 273–276.
Zajac, R., & Chakrabarti, A. (1995). Irreversible polymer adsorption from semidilute and moderately dense solutions. *Physical Review E*, *52*(6), 6536–6549.
Zhou, J. W., Ellis, A. V., & Voelcker, N. H. (2010). Recent developments in PDMS surface modification for microfluidic devices. *Electrophoresis*, *31*(1), 2–16.